# Minimum Time-Energy Pull-up Maneuvers for Airborne Launch Vehicles

Jiamin Zhu, Emmanuel Trélat, Max Cerf

# Minimum Time-Energy Pull-up Maneuvers for Airborne Launch Vehicles

Jiamin Zhu* Emmanuel Trélat† Max Cerf‡

**Résumé**

In this paper, the minimum time-energy pull-up maneuver problem for airborne launch vehicles (ALV) is studied with a focus on developing a numerical approach for solving the problem. Firstly, the six-degree-of-freedom (6DOF) dynamics for the motion of the ALV subject to the aerodynamic forces, the gravitational force, the propulsive force and the path constraints are established. Then, first-order necessary conditions are derived by applying the Pontryagin Maximum Principle, and the optimal control problem is transformed into a two-boundary value problem, which is generally solved numerically thanks to a shooting method. However, the convergence domain of the shooting method is very small due to high dimension and to nonlinear coupling of attitude and trajectory motions. To overcome this difficulty, we design an algorithm combining the multiple shooting method and the Predictor-Corrector continuation (PC continuation) method, where the choice of homotopy parameters relies on a careful analysis of the nature of the dynamics. Numerical results presented for pull-up maneuvers of an ALV show that the algorithm is efficient and robust with respect to terminal conditions. Our method is also applied to the problem of rapid maneuver of the upper stage of a launch vehicle (LV).

**Keywords :** coupled attitude trajectory problem ; optimal control ; Pontryagin maximum principle ; multiple shooting ; numerical continuation ; airborne launch vehicle ; path constraint.

## Nomenclature

| | | |
|---|---|---|
| $S_R = (\mathbf{x}_R, \mathbf{y}_R, \mathbf{z}_R)$ | = | launch frame |
| $S_b = (\mathbf{x}_b, \mathbf{y}_b, \mathbf{z}_b)$ | = | body frame |
| $S_v = (\mathbf{x}_v, \mathbf{y}_v, \mathbf{z}_v)$ | = | velocity frame |
| $\mathbf{r}$ | = | position vector (from the origin of $S_R$ towards the launcher), $m$ |
| $\mathbf{r}_d$ | = | vector from the origin of the Earth towards the launcher, $m$ |
| $\mathbf{v}$, $v$ | = | velocity vector, module of the velocity velocity, $m/s$ |
| $\mathbf{E} = (\theta, \psi, \phi)$ | = | Euler angles (pitch angle, yaw angle, roll angle), $rad$ |
| $\boldsymbol{\omega}$ | = | angular velocity vector, $rad/s$ |
| $\mathbf{I}_b$ | = | inertia matrix |
| $m$ | = | mass of the LV, $kg$ |

*Sorbonne Universités, UPMC Univ Paris 06, CNRS UMR 7598, Laboratoire Jacques-Louis Lions, F-75005, Paris, France (zhu@ann.jussieu.fr).

†Sorbonne Universités, UPMC Univ Paris 06, CNRS UMR 7598, Laboratoire Jacques-Louis Lions, Institut Universitaire de France, F-75005, Paris, France (emmanuel.trelat@upmc.fr).

‡Airbus Defence and Space, Flight Control Unit, 66 route de Verneuil, BP 3002, 78133 Les Mureaux Cedex, France (max.cerf@astrium.eads.net).

| | | |
|---|---|---|
| $\mathbf{g}$ | = | gravity acceleration vector, $m/s^2$ |
| $\mathbf{T}$ | = | thrust force vector, $N$ |
| $\mathbf{L}$ | = | lift force vector, $N$ |
| $\mathbf{D}$ | = | drag force vector, $N$ |
| $S$ | = | reference surface, $m^2$ |
| $C_x$,$C_{x0}$,$C_{x\alpha}$ | = | coefficients of the drag force |
| $C_z$,$C_{z0}$,$C_{z\alpha}$ | = | coefficients of the lift force |
| $R_E$ | = | radius of the Earth, $m$ |
| $\alpha$ | = | angle of attack, $rad$ |
| $\bar{n}$ | = | load factor |
| $\bar{q}$ | = | dynamic pressure, $kPa$ |
| $\xi$, $\kappa$ | = | flight path angle, bank angle, $rad$ |
| $u = (u_1, u_2)$ | = | control variable, $u \in \mathbb{R}^2$ |
| $x$ | = | state variable, $x \in \mathbb{R}^{11}$ |
| $p$ | = | adjoint variable, $p \in \mathbb{R}^{11}$ |
| $K$ | = | regularization parameter |
| $K_p$ | = | penalty parameter |

# 1 Introduction

Since the first successful flight of Pegasus vehicle in April 1990, the ALVs have always been a potentially interesting technique for small and medium-sized space transportation systems. The mobility and deployment of the ALVs provide increased performance and reduced velocity requirements due to non-zero initial velocity and altitude (see, e.g., [24, 25, 27, 44, 46]).

ALVs consist of a carrier aircraft and a rocket-powered LV. ALVs are typically started (several seconds) after they are dropped almost horizontally from the carrier aircraft for the safety of the carrier aircraft. In order to benefit from the airborne launch [45, 46], a pull-up maneuver is required to rotate the ALVs in order to attain the optimal release flight path angle ($30° \pm 15°$ for subsonic release velocities). Consider for example the Pegasus vehicle [3, 11, 38, 43]. It is released horizontally with an altitude of $12.65\,km$. Its first stage is ignited with an altitude of $12.54\,km$ and a velocity of $236.8\,m/s$ (0.8 Mach). Then it has to fulfill a pull-up maneuver until having a flight path angle of $13.8°$ (for the ignition of the second stage) subject to a maximal load factor of $2.5\,g$ and a maximal dynamic pressure of $47.6\,kPa$.

To tackle the pull-up maneuver problem for ALVs, the vehicle cannot be regarded as a single mass point, since the pull-up maneuver consists of performing an attitude maneuver such that the flight path angle increases up to its expected value, while being subject to path constraints. In this paper, we address the minimum time-energy pull-up maneuver problem for ALVs with a focus on the numerical resolution of the problem.

The problem consists of minimizing the cost functional

$$C(t_f, u) = t_f + K \int_0^{t_f} \|u(t)\|^2 \, dt \tag{1}$$

for the six-degree-of-freedom (6DOF) dynamical system

$$\dot{\mathbf{r}} = \mathbf{v}, \qquad \dot{\mathbf{v}} = \mathbf{g} + \frac{\mathbf{T} + \mathbf{L} + \mathbf{D}}{m}, \tag{2}$$

$$\dot{\mathbf{E}} = f_E(\mathbf{E}, \boldsymbol{\omega}), \qquad \mathbf{I}_b \dot{\boldsymbol{\omega}} = -\boldsymbol{\omega} \wedge \mathbf{I}_b \boldsymbol{\omega} + \mathbf{M}, \qquad \|\mathbf{M}\| \leqslant M_{max}, \tag{3}$$

with initial conditions

$$\mathbf{r}(0) = \mathbf{r}_0, \quad \mathbf{v}(0) = \mathbf{v}_0, \quad \mathbf{E}(0) = \mathbf{E}_0, \quad \boldsymbol{\omega}(0) = \boldsymbol{\omega}_0,$$

and final conditions

$$\mathbf{r}(t_f) \,\text{free}, \quad \mathbf{v}(t_f) \,/\!/\, f_z(\mathbf{E}, t_f), \quad \boldsymbol{\omega}(t_f) = \mathbf{0},$$

where $f_E : \mathbb{R}^3 \times \mathbb{R}^3 \mapsto \mathbb{R}^3$ is a nonlinear mapping, $\mathbf{M}$ is the control torque of which the module is bounded by a given $M_{max} > 0$, and $f_z(\mathbf{E}, t_f)$ represents the unit directional vector of the longitudinal axis of the launcher at time $t_f$. The first two equations describe respectively the trajectory kinematics and dynamics, and the last two equations describe the attitude kinematics and dynamics, respectively. In addition, path constraints on the load factor $\bar{n}$ and on the dynamic pressure $\bar{q}$ are required to be satisfied during the maneuver.

By applying the Pontryagin Maximum Principle (PMP; see, e.g., [41]), this optimal control problem can be reduced to a two-point boundary value problem. However, due to high dimension and to nonlinear coupling between aerodynamics, propulsion, vehicle attitude and trajectory, usual numerical shooting methods for solving this two-point boundary value problem are very hard to initialize successfully. Therefore, it is required to combine them with other theoretical or numerical approaches (see the survey [48]). The numerical continuation (also called homotopy method) is a powerful tool that can be combined with indirect shooting methods. The idea of *continuation* is to solve a problem step by step from a simpler problem by parameter deformation (see, e.g., [1]). For example, in [10, 21, 36], the continuation method is used to solve orbit transfer problems, and in [4, 9, 20, 29] continuation procedures are used to introduce atmospheric effects and path constraint terms related to the endo-atmospheric LV ascent problem, starting from a nearly analytic vacuum solution.

Therefore, in view of successfully solving the pull-up maneuver problem, we propose to combine the multiple shooting method with the PC continuation method. Note that we use here a multiple (instead of single) shooting method in order to obtain a better numerical stability. The continuation procedure is designed from on a careful analyis of the specific structure of the problem, leading to an adequate choice of the homotopy parameters. An important property is the coupling of the attitude motion (which is fast) with the trajectory motion (which is slow). On the one hand, this property causes difficulties in numerical approaches, especially in indirect methods where Newton-like algorithms are implemented to address the boundary value problem. On the other hand, this coupling property suggests that singular perturbation theory (see, e.g., [2, 6, 12, 28, 39]) may be relevant in our context.

We first analytically solve what we call the problem of order zero, which consists of calculating the time optimal solution of the trajectory velocity reorientation using Euler angles as control inputs. Then, we use a continuation procedure to re-introduce the desired attitude terminal conditions, the aerodynamic forces and the terms induced by path constraints. Our approach turns out to be time-efficient and an advantage is that our method does not need user-supplied initial guesses. In addition, we show how our study and design methodology apply as well to attitude reorientation for LVs.

The paper is organized as follows. In Section 2, we establish the 6DOF model of pull-up maneuvers and we apply the PMP to the formulated optimal control problem. In Section 3, we recall the multiple shooting and PC continuation methods, we define the problem of order zero. Then, we describe the continuation procedure, and we use a frame transformation and a smoothing of the vector fields to enhance the continuation strategy. Finally, in Section 3, numerical results are given, including an example of ALV minimum time-energy pull-up maneuver, statistical results for pull-up maneuvers of an ALV, and an example of rapid maneuver for a LV.

# 2 Problem statement and application of the PMP

## 2.1 The model

Throughout the paper, we make the following assumptions : the Earth is a sphere and is fixed in the inertial space ; the engine cannot be shut off during the maneuver, and the module of the thrust force is constant, taking its maximal value ; the mass $m$ is constant.

**Coordinate systems.** All coordinate systems introduced here are Cartesian.

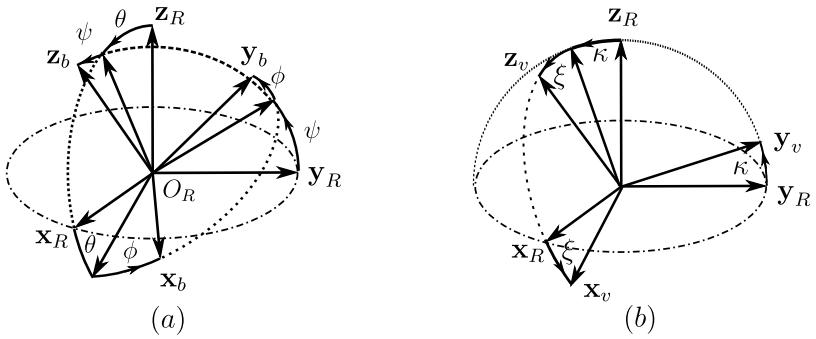


FIGURE 1 – Coordinate systems and relations.

The launch (reference) frame $S_R$ is fixed around the launch point $O_R$. The axis $\mathbf{x}_R$ points radially outwards (normal to the local tangent plane), and the axis $\mathbf{z}_R$ points to the North.

The body frame $S_b$ is defined as follows. The origin of the frame $O_b$ is fixed around the mass center of the launcher, the axis $\mathbf{z}_b$ is along the longitudinal axis of the launcher, and the axis $\mathbf{x}_b$ is in the cross-section. As shown in Fig. 1 (a), the body frame can be derived by three ordered unit single-axis rotations from the launch frame,

$$S_R \xrightarrow{R_y(\theta)} \circ \xrightarrow{R_x(\psi)} \circ \xrightarrow{R_z(\phi)} S_b,$$

where $R_j(k)$ is a rotation of the frame around the axis $j \in \{x, y, z\}$ with an angle $k \in \mathbb{R}$. Therefore, the transfer matrix from $S_b$ to $S_R$ is $L_{Rb} = L_{bR}^\top = R_y(\theta)^\top R_x(\psi)^\top R_z(\phi)^\top$.

The velocity frame $S_v$ is fixed around the mass center of the launcher. The axis $\mathbf{x}_v$ is parallel to the velocity vector, and the axis $\mathbf{z}_v$ is normal to the velocity, pointing to the direction of the lift force $\mathbf{L}$. This frame can be derived by two unit single-axis rotations from the launch frame as shown in Fig. 1 (b),

$$S_R \xrightarrow{R_x(\kappa)} \circ \xrightarrow{R_y(\xi)} S_v.$$

We consider the projection of $\mathbf{v}$ in the $S_R$ frame, $(\mathbf{v})_R = (v_x, v_y, v_z)^\top$. Since $v_x = v\cos\xi$, $v_y = v\sin\xi\sin\kappa$, $v_z = -v\sin\xi\cos\kappa$, we have $\cos\xi = v_x/v$, and $\tan\kappa = -v_y/v_z$ if $\sin\xi \neq 0$.

For convenience, we define $\theta_v$ and $\psi_v$ as the "pitch" and "yaw" angles of the velocity vector, and thus we also have $v_x = v\sin\theta_v\cos\psi_v$, $v_y = -v\sin\psi_v$, $v_z = v\cos\theta_v\cos\psi_v$. Then, we get $\tan\theta_v = 1/\tan\xi\cos\kappa$ and $\sin\psi_v = -\sin\xi\sin\kappa$. Moreover, the transfer matrix from $S_v$ to $S_R$ is $L_{Rv} = L_{Rv}^\top = R_x(\kappa)^\top R_y(\xi)^\top$.

Throughout the paper, for any vector $x \in \mathbb{R}^3$, $(x)_w$ is the projection of this vector in the frame $S_w \in \{S_R, S_b, S_v\}$, $\langle\cdot,\cdot\rangle$ is the inner product of two vectors, and $\|\cdot\|$ is the $L_2$-norm.

**Attitude motion equations.** Assume that $\mathbf{I}_b = \mathrm{diag}(I_x, I_y, I_z)$ and $I_x = I_y$. Set $(\omega)_b = (\omega_x, \omega_y, \omega_z)^\top$, and assume that $\omega_z = 0$ (due to the fact that the deflection of the thrust with respect to the longitudinal axis of the launcher does not provide a rotation torque around the longitudinal axis). Then, we can write Eqs. (3) in the $S_b$ frame as

$$\begin{aligned} &\dot\theta = (\omega_x \sin\phi + \omega_y \cos\phi)/\cos\psi, \quad \dot\psi = \omega_x \cos\phi - \omega_y \sin\phi, \quad \dot\phi = (\omega_x \sin\phi + \omega_y \cos\phi)\tan\psi, \\ &\dot\omega_x = -bu_2, \quad \dot\omega_y = bu_1, \end{aligned} \tag{4}$$

where $b = \mu_{max} T_{max} l/(2I_x)$, $T_{max}$ is the maximal thrust module, $\mu_{max}$ is the maximal thrust deflection between $\mathbf{T}$ and $\mathbf{z}_b$, and $l$ is length of the LV (see [52] for more details).

Note that, when $\psi = \pi/2 + k\pi$ ($k \in \mathbb{Z}$), the system encounters singularities due to the fact that the Euler angle $\phi$ is not well defined at such points. We call these points *Euler singularities* for convenience. We will see in Section 3 numerical tips to deal with these singularities.

**Trajectory motion equations.** According to our assumptions, we have

$$(\mathbf{T})_R = T_{max}(\sin\theta\cos\psi, -\sin\psi, \cos\theta\cos\psi)^\top.$$

Setting $\mathbf{R}_E = (R_E, 0, 0)^\top$, we have $\mathbf{r}_d = \mathbf{r} + \mathbf{R}_E$, and the gravity acceleration vector $\mathbf{g}$ is given by

$$(\mathbf{g}(t))_R = \left(\mathbf{g}_0 \frac{\|\mathbf{r}_d(0)\|^2}{\|\mathbf{r}_d(t)\|}\right)_R = (g_x, g_y, g_z)^\top, \tag{5}$$

where $\mathbf{g_0}$ is the gravity acceleration at the origin of the frame $S_R$.

Denoting the air density by $\rho$, the drag and lift forces are expressed in the frame $S_v$ by $(\mathbf{D})_v = (-\frac{1}{2}\rho v^2 S C_x, 0, 0)^\top$ and $(\mathbf{L})_v = (0, 0, \frac{1}{2}\rho v^2 S C_z)^\top$. We consider an exponential atmospheric density model. The aerodynamic coefficients are approximated by $C_x = C_{x0} + C_{x\alpha}\alpha^2$ and $C_z = C_{z0} + C_{z\alpha}\alpha$, where $C_{x0}$, $C_{x\alpha}$, $C_{z0}$ and $C_{z\alpha}$ are constant coefficients. Then, by using the transfer matrix $L_{Rv}$, we get

$$\begin{aligned} (\mathbf{D})_R = (D_x, D_y, D_z)^\top &= \frac{1}{2}\rho S C_x v^2 (-\cos\xi, -\sin\xi\sin\kappa, \sin\xi\cos\kappa)^\top, \\ (\mathbf{L})_R = (L_x, L_y, L_z)^\top &= \frac{1}{2}\rho S C_z v^2 (\sin\xi, -\cos\xi\sin\kappa, \cos\xi\cos\kappa)^\top. \end{aligned}$$

Therefore, Eqs. (2) can be written in the $S_R$ frame as

$$\begin{aligned} &\dot r_x = v_x, \qquad \dot r_y = v_y, \qquad \dot r_z = v_z, \\ &\dot v_x = a\sin\theta\cos\psi + g_x + D_x/m + L_x/m, \\ &\dot v_y = -a\sin\psi + g_y + D_y/m + L_y/m, \\ &\dot v_z = a\cos\theta\cos\psi + g_z + D_z/m + L_z/m, \end{aligned} \tag{6}$$

where $a = T_{max}/m$ is constant.

**Inequality state constraint.** During the atmospheric flight, the lateral load factor due to aerodynamic forces must be limited according to

$$\bar n = \frac{\bar q S C_N}{m g_0} = \frac{\rho \|v\|^2 S C_N}{2 m g_0} \leqslant \bar n_{max},$$

where $\bar q$ is the dynamic pressure and $\bar n_{max}$ is the maximal admissible load factor. The coefficient $C_N$ is approximated by $C_N = C_{N0} + C_{N\alpha}\alpha$. Note that

$$\begin{pmatrix} C_z \\ C_x \end{pmatrix} = \begin{pmatrix} \cos\alpha & -\sin\alpha \\ \sin\alpha & \cos\alpha \end{pmatrix} \begin{pmatrix} C_N \\ C_A \end{pmatrix},$$

where the angle of attack $\alpha$ is defined by $\alpha = (v_x \sin\theta\cos\psi - v_y \sin\psi + v_z \cos\theta\cos\psi)/v$. We also require that the dynamic pressure be bounded above by a maximal value $\bar{q}_{max}$, i.e., $\bar{q} \leqslant \bar{q}_{max}$.

Defining the state $x = (r_x, r_y, r_z, v_x, v_y, v_z, \theta, \psi, \phi, \omega_x, \omega_y)$, the above constraints can be formulated as inequality state constraints for our optimal control problem, in the form

$$c(x) = (c_1(x), c_2(x))^\top = (n - n_{max}, \bar{q} - \bar{q}_{max})^\top \leqslant 0. \tag{7}$$

The system (4)-(6) can be written as the bi-input control-affine system $\dot{x} = f(x) + u_1 g_1(x) + u_2 g_2(x)$, where the control satisfies the constraint $\|u\| = \sqrt{u_1^2 + u_2^2} \leqslant 1$, and $f$, $g_1$ and $g_2$ are smooth vector fields. If $b$ is a function and $Z$ is a vector field, then $Z$ acts on $b$ by Lie derivative $Z.b = \frac{\partial b}{\partial x}(x)Z(x)$. Recall that a state constraint $c(x) \leqslant 0$ (also called path constraint) is of order $m$ if $g_i.c = g_i f.c = \cdots = g_i f^{m-2}.c = 0$ and $g_i f^m.c \neq 0$, $i = 1, 2$. A boundary arc is an arc (not reduced to a point) solution of the system satisfying $c(x(t)) = c^{(1)}(x(t)) = \cdots = c^{(m-1)}(x(t)) = 0$, and the control along the boundary arc is a feedback control calculated by solving $c^{(m)} = f^m.c + u_1\, g_1 f^{(m-1)}.c + u_2\, g_2 f^{(m-1)}.c = 0$. Here, we find that the constraint on the load factor $\bar{n}$ is of order 2 and the constraint on the dynamic pressure $\bar{q}$ is of order 3. We will see that such a state constraint is difficult to tackle numerically if we consider it as a hard constraint, and we will propose to use a soft constraint method.

**Pull-up maneuver problem.** The desired final velocity is required to be parallel to the longitudinal axis $\mathbf{z}_b$, that is, $(\mathbf{v}(t_f))_R \wedge (\mathbf{z}_b(t_f))_R = \mathbf{0}$. This requirement reflects the fact that most launchers are planned to maintain a zero angle of attack along the flight.

We set $x_0 = (r_{x0}, r_{y0}, r_{z0}, v_{x0}, v_{y0}, v_{z0}, \theta_0, \psi_0, \phi_0, \omega_{x0}, \omega_{y0})$ and we define the target set

$$\begin{aligned} M_1 = \{&(r_x, r_y, r_z, v_x, v_y, v_z, \theta, \psi, \phi, \omega_x, \omega_y) \in \mathbb{R}^{11} \;\mid\; \theta = \theta_f, \quad \psi = \psi_f, \quad \phi = \phi_f, \\ &v_z \sin\psi_f + v_y \cos\theta_f \cos\psi_f = 0, \quad v_z \sin\psi_f + v_y \cos\theta_f \cos\psi_f = 0, \quad \omega_x = \omega_{xf}, \quad \omega_y = \omega_{yf}\}. \end{aligned}$$

The *pull-up maneuver problem* consists of steering the system (4)-(6) from $x(0) = x_0$, i.e., from

$$\begin{aligned} &r_x(0) = r_{x0}, \quad r_y(0) = r_{y0}, \quad r_z(0) = r_{z0}, \quad v_x(0) = v_{x_0}, \quad v_y(0) = v_{y_0}, \quad v_z(0) = v_{z_0}, \\ &\theta(0) = \theta_0, \quad \psi(0) = \psi_0, \quad \phi(0) = \phi_0, \quad \omega_x(0) = \omega_{x0}, \quad \omega_y(0) = \omega_{y0}, \end{aligned} \tag{8}$$

to some final point belonging to the target $M_1$, i.e., such that

$$\begin{aligned} &v_{zf} \sin\psi_f + v_{yf} \cos\theta_f \cos\psi_f = 0, \quad v_{zf} \sin\theta_f - v_{xf} \cos\theta_f = 0, \\ &\theta(t_f) = \theta_f, \quad \psi(t_f) = \psi_f, \quad \phi(t_f) = \phi_f, \quad \omega_x(t_f) = \omega_{xf}, \quad \omega_y(t_f) = \omega_{yf}. \end{aligned} \tag{9}$$

while minimizing the cost functional $C$ defined by (1), over all possible controls satisfying the control constraint $\|u\| = \sqrt{u_1^2 + u_2^2} \leqslant 1$ and whose corresponding trajectories satisfy the state inequality constraints (7). We denote this pull-up maneuver problem by $\mathbf{(PUP)}_K$ in the sequel.

## 2.2 Application of the Pontryagin maximum principle

**Hard constraint formulation.** According to the PMP with state constraints (see, e.g., [22]), there exists a nontrivial triple of Lagrangian multipliers $(p, p^0, \eta)$, with $p^0 \leqslant 0$, $p \in BV(0, t_f)^{11}$ and $\eta = (\eta_1, \eta_2) \in BV(0, t_f)^2$, where $BV(0, t_f)$ is the set of functions of bounded variation over $[0, t_f]$, such that

$$\dot{x} = \frac{\partial H(x, p, u, p^0, \eta)}{\partial p}, \qquad dp = -\frac{\partial H(x, p, u, p^0, \eta)}{\partial x} dt - \sum_{i=1}^{2} \frac{\partial c_i(x)}{\partial x} d\eta_i,$$

almost everywhere on $[0, t_f]$, where the Hamiltonian of the problem is $H(x, p, u, p^0, \eta) = \langle p, f(x) + u_1 g_1(x) + u_2 g_2(x)\rangle + \sum_{i=1}^{2} \eta_i c_i(x) + p^0(1 + K\|u\|^2)$, and we have the maximization condition $u(t) \in \operatorname{argmax}_w H(x(t), p(t), w, p^0, \eta(t))$ for almost every $t$. In addition, we have $d\eta_i \geqslant 0$ and $\int_0^{t_f} c_i(x)\, d\eta_i = 0$ for $i = 1, 2$.

Along a boundary arc, we must have $h_i = \langle p, g_i(x)\rangle = 0$, $i = 1, 2$. Assume that only the first constraint (which is of order 2) is active along this boundary arc. Then by differentiating two times the switching functions $h_i$, $i = 1, 2$, we have $d^2 h_i = \langle p, \mathrm{ad}^2 f.g_i(x)\rangle dt^2 - d\eta_1 \cdot (\mathrm{ad} f.g_i).c_1 dt$. Moreover, at an entry point, letting $t = \tau$, we have $dh_i(\tau^+) = dh_i(\tau^-) - d\eta_1 \cdot (\mathrm{ad} f.g_i).c_1 = 0$. Hence we can calculate $d\eta_1$. A similar result is obtained at an exit point.

The main drawback of this hard constraint formulation is that it does not provide a solution if the state is perturbed in the constrained region [26]. Moreover, the adjoint vector $p$ is no longer absolutely continuous : a jump $d\eta$ may occur at the entry or at the exit point of a boundary arc. Then, in order to design a robust algorithm for solving the problem $\mathbf{(PUP)}_K$, we will use another approach.

An alternative to treat the dynamic pressure state constraint, used in [13, 16, 29], is to design a feedback law that reduces the commanded throttle based on an error signal. According to [16], this approach works well when the trajectory does not violate too much the maximal dynamic pressure constraint. In contrast, if the constraint is violated significantly, this approach may cause instability in the flight. Moreover, the derived solutions are suboptimal.

Another alternative is the *soft constraint method* (also called *penalty function method*). According to [26], the hard constraints could be problematic when using singular perturbation method if the trajectory is perturbed in a constrained region, whereas the soft constraint does not have this problem. The soft constraint is implemented using a penalty function to discard solutions entering the constrained region [14, 35].

For the problem $\mathbf{(PUP)}_K$, we adopt the soft constraint method, because unconstrained solutions for ALV flights generally violate significantly the state constraint, and the continuation procedure that we will use is actually starting from a solution lying in the constrained region.

**Soft constraint formulation.** Following the soft constraint method, the constraint problem $\mathbf{(PUP)}_K$ is recast as an unconstrained optimal control problem by adding a penalty function to the cost functional, i.e.,

$$C(t_f, u, K_p) = t_f + K \int_0^{t_f} \|u\|^2 dt + K_p \int_0^{t_f} P(x(t)) dt, \tag{10}$$

where the penalty function $P(\cdot)$ for the state inequality constraint (7) is given by

$$P(x) = \begin{cases} 0 & \text{if } \bar{n} < \bar{n}_{max}, \\ (\bar{n} - \bar{n}_{max})^2 + (\max(0, \bar{q} - \bar{q}_{max}))^2 & \text{if } \bar{n} \geqslant \bar{n}_{max}, \end{cases}$$

Tuning the parameter $K_p$ allows one to control the constraint violation. Then, we apply the PMP to this "unconstrained" problem. We still denote this unconstrained problem by $\mathbf{(PUP)}_K$.

**Application of the PMP without state constraint.** The Hamiltonian is now given by $H(x, p, p^0, u) = \langle p, f(x)\rangle + u_1\langle p, g_1(x)\rangle + u_2\langle p, g_2(x)\rangle + p^0(1 + K\|u\|^2 + K_p P(x))$. Here we assume $p^0 = -1$ (normal case, see [52]). The adjoint equation is

$$\dot{p}(t) = -\frac{\partial H}{\partial x}(x(t), p(t), p^0, u(t)), \tag{11}$$

where we have set $p = (p_{r_x}, p_{r_y}, p_{r_z}, p_{v_x}, p_{v_y}, p_{v_z}, p_\theta, p_\psi, p_\phi, p_{\omega_x}, p_{\omega_y})$. Let $h = (h_1, h_2)$ be the switching function and let $h_1(t) = \langle p(t), g_1(x(t))\rangle = b p_{\omega_y}(t)$ and $h_2(t) = \langle p(t), g_2(x(t))\rangle = -b p_{\omega_x}(t)$. The maximization condition of the PMP gives

$$u = \begin{cases} (h_1, h_2)/(2K) & \text{if } \|h\| \leqslant 2K, \\ (h_1, h_2)/\|h\| & \text{if } \|h\| > 2K. \end{cases} \tag{12}$$

Moreover, the transversality condition $p(t_f) \perp T_{x(t_f)}M_1$, where $T_{x(t_f)}M_1$ is the tangent space to $M_1$ at the point $x(t_f)$, yields the additional conditions $p_{vy}(t_f)\sin\psi_f = p_{vx}(t_f)\sin\theta_f\cos\psi_f + p_{vz}(t_f)\cos\theta_f\cos\psi_f$ and $p_{r_x}(t_f) = p_{r_y}(t_f) = p_{r_z}(t_f) = 0$. The final time $t_f$ being free and the system being autonomous, we have in addition that $H(x(t), p(t), -1, u(t)) = 0$ almost everywhere on $[0, t_f]$.

We say that the optimal control given by Eq. (12) is regular. When $K = 0$ and $\|h(t)\| = 0$, the control is said *singular*. We refer to [52] for the precise calculation of singular controls in our problem. Note that the term $K\int_0^{t_f}\|u(t)\|^2 dt$ in the cost functional (10) is used to avoid chattering [34, 18, 42, 50, 51, 52], and the exact minimum time solution can be approached by decreasing step by step the value of $K \geqslant 0$.

**Remark 1** (Choice of the penalty parameter.)**.** According to the cost functional defined by (10), we see that if $K_p$ is small compared with the other two terms, minimizing $C(t_f, u, K_p)$ may not produce a feasible solution. Therefore, the penalty parameter $K_p$ should be chosen large enough. However, large values of $K_p$ may create steep valleys at the constraint boundaries, which raise difficulties for search methods. In order to choose an adequate value for $K_p$, a simple strategy [19, 47] is to start with a quite small value of $K_p = K_{p0}$ and then to increase $K_p$ while solving a sequence of problems until reaching a quite large $K_p = K_{p1}$. We stop increasing $K_p$ when $\|c(x(t))\| < \epsilon_c$, for every $t \in [0, t_f]$, for some given tolerance $\epsilon_c > 0$.

# 3 Resolution algorithm

In this section, we first define what we call the *problem of order zero*, denoted by (**OCP0**), the solution of which can be easily computed. Then we embed this simple, low-dimensional solution into higher dimension, in order to initialize an indirect method (multiple shooting) for the more complex problem $\mathbf{(PUP)}_K$.

Before providing the details of our approach, we first briefly recall what are the multiple shooting method and the Predictor-Corrector (PC) continuation method that we will then use to ensure efficiency and robustness of our algorithm.

## 3.1 Multiple shooting and PC continuation methods

### 3.1.1 Multiple shooting method

Compared with a single shooting method, the multiple shooting has a better numerical stability. The multiple shooting approach has also been used to solve the optimal multi-burn ascent problem (see [15, 16, 30, 31, 32, 33, 40]). It consists in dividing the interval $[0, t_f]$ into $N$ subintervals $[t_i, t_{i+1}]$ and in considering as unknowns the values of $z_i = (x(t_i), p(t_i))$ at the beginning of each subinterval. The application of the PMP to the optimal control problem yields a multi-point boundary value

problem, consisting of finding $Z = (p(0), t_f, z_i)$, $i = 1, \cdots, N-1$, such that the differential equation

$$\dot{z}_i(t) = F(z(t)) = \begin{pmatrix} \frac{\partial H(x,p,p^0,u(x,p))}{\partial p} \\ -\frac{\partial H(x,p,p^0,u(x,p))}{\partial x} \end{pmatrix} = \begin{cases} F_0(z(t)) & \text{if } t_0 \leqslant t \leqslant t_1, \\ F_1(z(t)) & \text{if } t_1 \leqslant t \leqslant t_2, \\ \vdots & \\ F_{N-1}(z(t)) & \text{if } t_{N-1} \leqslant t \leqslant t_f, \end{cases}$$

and the constraints $x(0) = x_0$, $x(t_f) \in M_1$, $H(t_f) = 0$, $p(t_f) \perp T_{x(t_f)}M_1$, and $z(t_i^-) = z(t_i^+)$, $i = 1, \cdots, N-1$, are satisfied. This problem can be solved by iterative methods, for example, a Newton type method. The nodes of the multiple shooting method may involve the switching times (at which the switching function changes its sign), and the junction times (entry, contact, or exit times) with boundary arcs. In this case it is required to have an a priori knowledge of the structure of the optimal solution. In the absence of any information on the optimal solution, we implement the multiple shooting method with a regular subdivision, i.e., $t_i = i\frac{t_f}{N}$ for $i = 1, \cdots, N-1$.

### 3.1.2 Predictor-Corrector continuation method

Let $n_h$ be the number of unknowns of the multiple shooting method (dimension of $Z$). Let $G : \mathbb{R}^{n_h} \times \mathbb{R} \mapsto \mathbb{R}^{n_h}$ be a deformation such that $G(Z, 0) = G_0(Z)$ and $G(Z, 1) = G_1(Z)$, where $G_1 : \mathbb{R}^{n_h} \mapsto \mathbb{R}^{n_h}$ is the smooth map of which one wants to determine the zeros points, and $G_0 : \mathbb{R}^{n_h} \mapsto \mathbb{R}^{n_h}$ is a smooth map for which the determination of its zeros is easy. Denote the continuation parameter by $\lambda$, then by discretizing $\lambda$ by $0 = \lambda^0 < \lambda^1 < \cdots < \lambda^{n_l} = 1$ and solving a sequence of problems $G(Z, \lambda^i) = 0$, $i = 1, \cdots, n_l$, one will generally be able to find the zeros of $G_1(Z)$. The reason is that if the increment $\triangle\lambda = \lambda^{i+1} - \lambda^i$ is small enough, then the solution $Z^i$ corresponding to $\lambda^i$ is expected to be close to the solution of $G(Z, \lambda^{i+1}) = 0$.

However, the parameter $\lambda$ can be ill suited as a parametrization for the zero curve $(Z, \lambda) \in \{(Z, \lambda) \mid G(Z, \lambda) = 0\}$, and it is explained in [1] that the arc-length, which is a natural parameter for the curve, can be a better choice for parametrization. On the model of the differential continuation method implemented in [7], which consists of integrating the zero curve, here we implement a Predictor-Corrector method which is computationally easier for our problem (see details in [1]).

We parameterize the zero curve by arc length $s$ and we denote the zero curve by $c_h(s) = (Z(s), \lambda(s))$. Denote $\frac{\partial G(Z(s),\lambda(s))}{\partial(Z,\lambda)}$ and $\frac{dc_h(s)}{ds}$ by $J_G$ and $t(J_G)$, respectively. Differentiating $G(Z(s), \lambda(s)) = 0$ with respect to $s$, we have $J_G\, t(J_G) = 0$, $\|t(J_G)\| = 1$, $c_h(Z(0), 0) = (Z(0), 0)$. Assume that $c_h(s)$ is not critical and assume that we know a point of this curve $(Z(s_i), \lambda(s_i))$. Then we predict a zero point $(\tilde{Z}(s_{i+1}), \tilde{\lambda}(s_{i+1}))$ by

$$(\tilde{Z}(s_{i+1}), \tilde{\lambda}(s_{i+1})) = (Z(s_i), \lambda(s_i)) + h_s\, t(J_G), \tag{13}$$

where $h_s$ is a given step size of $s$. When the step size $h_s$ is small enough, the point $(\tilde{Z}(s_{i+1}), \tilde{\lambda}(s_{i+1}))$ may be very close to the solution point $(Z(s_{i+1}), \lambda(s_{i+1})) = G^{-1}(c_h(s_{i+1})) = 0$, and thus makes the Newton type iterative method (serving as a corrector) easier to converge. However, calculating the Jacobian matrix $J_G$ might be computationally heavy, and thus we use an approximation. According to [8], the first turning point of $\lambda(\bar{s})$ (where $\frac{d\lambda}{ds}(\bar{s}) = 0$ and $\frac{d^2\lambda}{ds^2}(\bar{s}) \neq 0$) corresponds to a conjugate point (the first point where extremals lose local optimality) at time $t_f$. By contraposition, if we assume the absense of the conjugate point, then there is no turning point in $\lambda(s)$, and then $\lambda$ increases monotonically along the zero path. Assume that we know three zeros $(Z_{i-2}, \lambda_{i-2})$, $(Z_{i-1}, \lambda_{i-1})$ and $(Z_i, \lambda_i)$, and let $s_1 = \|(Z_{i-1}, \lambda_{i-1}) - (Z_{i-2}, \lambda_{i-2})\|$, $s_2 = \|(Z_i, \lambda_i) - (Z_{i-2}, \lambda_{i-2})\|$, $s_3 = \|(Z_i, \lambda_i) - (Z_{i-1}, \lambda_{i-1})\|$, then we approximate $t(J_G)$ by

$$t(J_G) = \frac{(Z_i, \lambda_i) - (Z_{i-1}, \lambda_{i-1})}{s_2 - s_1} \frac{|s_2 - s_1|}{|s_3|}.$$

We note that when the when the step length $h_s$ is small enough, the predicted point (13) with this approximation is very close to the true zero.

## 3.2 Resolution algorithm

The objective is to compute the optimal solution of the problem $\mathbf{(PUP)}_K$, starting from the explicit solution of a simpler problem denoted by (**OCP0**). For convenience, we define the *exo-atmospheric pull-up maneuver problem* (**EPUP**) as the pull-up maneuver problem without state inequality constraints and without aerodynamic forces. Moreover, we define the *unconstrained pull-up maneuver problem* (**UPUP**) as the pull-up maneuver problem without state inequality constraints.

### 3.2.1 Problem of Order Zero

We define the *problem of order zero*, as a "subproblem" of the problem $\mathbf{(PUP)}_K$, in the sense that we consider only the trajectory motion and that we assume the attitude (Euler) angles able to take instantaneously any desired value. In other words, the Euler angles are considered as control inputs in that simpler problem. Meanwhile, we assume that the aerodynamic forces are zero and the gravity acceleration is constant. We formulate the problem as

$$\min t_f, \quad s.t. \quad \dot{\mathbf{r}} = \mathbf{v}, \quad \dot{\mathbf{v}} = a\mathbf{z}_b + \mathbf{g}_0, \quad \mathbf{r}(0) = \mathbf{r}_0, \quad \mathbf{v}(0) = \mathbf{v}_0, \quad \mathbf{v}(t_f) \;/\!/\; \mathbf{w}, \quad \|\mathbf{w}\| = 1,$$

where $\mathbf{w}$ is the desired target velocity direction. This problem is easy to solve, and the explicit solution derived by applying the PMP is given by

$$\mathbf{z}_b^* = \frac{1}{a}\left(\frac{k\mathbf{w} - \mathbf{v}_0}{t_f} - \mathbf{g}_0\right), \quad t_f = \frac{-a_2 + \sqrt{a_2^2 - 4a_1a_3}}{2a_1}, \quad p_r = \mathbf{0}, \quad p_v = \frac{-p^0}{a + \langle \mathbf{z}_b^*, \mathbf{g}_0\rangle}\mathbf{z}_b^*.$$

with $k = \langle \mathbf{v}_0, \mathbf{w}\rangle + \langle \mathbf{g}_0, \mathbf{w}\rangle t_f$, $a_1 = a^2 - \|\langle \mathbf{g}_0, \mathbf{w}\rangle \mathbf{w} - \mathbf{g}_0\|^2$, $a_2 = 2(\langle \mathbf{v}_0, \mathbf{w}\rangle\langle \mathbf{g}_0, \mathbf{w}\rangle - \langle \mathbf{v}_0, \mathbf{g}_0\rangle)$, and $a_3 = -\|\langle \mathbf{v}_0, \mathbf{w}\rangle \mathbf{w} - \mathbf{v}_0\|^2$. Since the solution $\mathbf{z}_b^*$ projects in the launch frame $S_R$ onto

$$(\mathbf{z}_b^*)_R = (\sin\theta^* \cos\psi^*, -\sin\psi^*, \cos\theta^* \cos\psi^*)^\top = (e_x^*, e_y^*, e_z^*),$$

the Euler angles $\theta^* \in (-\pi, \pi)$, $\psi^* \in (-\pi/2, \pi/2)$ are

$$\theta^* = \operatorname{atan2}(e_x^*, e_z^*), \quad \psi^* = \arcsin(-e_y^*). \tag{14}$$

Recall that, if $\psi = \pm\pi/2 + k\pi$, $k \in \mathbb{Z}$, then the Euler angles are not well defined. Then, if $\psi_0$ and $\psi_f$ are close $\pm\pi/2$, we perform in Section 3.3 a change of frame $S_R$ to a new reference frame $S'_R$. The Euler singularities are also treated in Section 3.4 by smoothing the vector field at such singular points.

Given a real number $\phi^*$, the optimal solution of (**OCP0**) actually corresponds to a singular solution of $\mathbf{(PUP)}_K$ with terminal conditions given by

$$\mathbf{v}(0) = \mathbf{v}_0, \quad \mathbf{E}(0) = \mathbf{E}^*, \quad \boldsymbol{\omega}(0) = \boldsymbol{\omega}^*, \tag{15}$$

$$\begin{gathered} v_z(t_f)\sin\psi_f + v_y(t_f)\cos\theta_f\cos\psi_f = 0, \quad v_z(t_f)\sin\theta_f - v_x(t_f)\cos\theta_f = 0, \\ \mathbf{E}(t_f) = \mathbf{E}^*, \quad \boldsymbol{\omega}(t_f) = \boldsymbol{\omega}^*, \end{gathered} \tag{16}$$

where $\mathbf{E}^* = (\theta^*, \psi^*, \phi^*)$, and $\boldsymbol{\omega}^* = \mathbf{0}$.

It is worth noting that this solution lies on the singular surface of $\mathbf{(PUP)}_{K=0}$, meaning that it is on the "highway" between two given points/submanifolds in the state space. On this "highway",

the system state goes the most rapidly towards the target point or manifold. Indeed, we observe in the numerical results that singular extremals of $\mathbf{(PUP)}_{K=0}$ play a role similar to that of stable points in the "turnpike" phenomenon described in [49] : optimal trajectories first tend to reach the singular surface (to have a greater speed in state transfer), then stay in the singular surface for a while until they are sufficiently close to the target submanifold $M_1$, and finally get off the singular surface to reach the target submanifold. Note that a singular arc is not necessary if the state is sufficiently close to the target.

We note again that the regularization term $K \int_0^{t_f} \|u\|^2 dt$ with $K > 0$ is necessary. Since the solution of (**OCP0**) is contained in the singular surface (filled by the singular solutions) for $\mathbf{(PUP)}_{K=0}$, passing directly from the solution of (**OCP0**) to the one of $\mathbf{(PUP)}_{K=0}$ forces optimal extremals to contain a singular arc (and thus chattering arcs), and the shooting method is then bound to fail due to numerical integration of a highly discontinuous Hamiltonian system.

### 3.2.2 Numerical strategy

We proceed as follows :

— First, we embed the solution of (**OCP0**) into the higher dimensional problem $\mathbf{(PUP)}_K$. For convenience, we still denote by (**OCP0**) the problem (**OCP0**) seen in higher dimension.

— Then, we pass from (**OCP0**) to $\mathbf{(PUP)}_K$ by using a numerical continuation procedure, involving four continuation parameters : two parameters $\lambda_1$ and $\lambda_2$ are used to introduce the terminal conditions (8)-(9) in **(EPUP)** ; $\lambda_3$ is used to introduce aerodynamic forces and variational gravity acceleration in **(UPUP)** ; $\lambda_4$ is used to introduce soft constraints in $\mathbf{(PUP)}_K$.

The overall continuation procedure is pictured in Fig. 2. We note that the procedure of decreasing $K$ is optional, but it is somehow important when dealing with the maneuver problem of the upper stage of LVs, since in that case a maneuver within smaller time is to be expected.

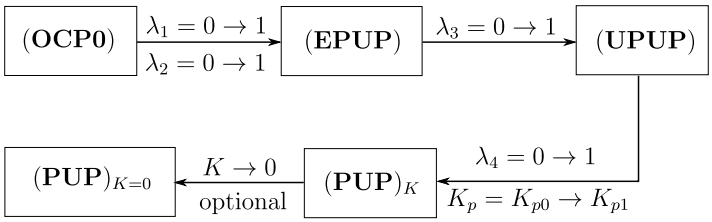


FIGURE 2 – Continuation procedure.

The unknowns of the shooting problem are $p(0) \in \mathbb{R}^{11}$, $t_f$ and $z_i \in \mathbb{R}^{22}$, $i = 1, \cdots, N-1$, where $z_i$ are the node points of the multiple shooting method. We set $Z = (p(0), t_f, z_i)$.

In the following, we call $\lambda_i$-continuation the continuation step corresponding to parameter $\lambda_i$, and we denote the shooting function for the $\lambda_i$-continuation step by $G_{\lambda i} = G(Z, \lambda_i)$.

We set $p_r = (p_{r_x}, p_{r_y}, p_{r_z})$, $p_E = (p_\theta, p_\psi, p_\phi)$, $p_\omega = (p_{\omega_x}, p_{\omega_y})$, $\phi^* = 0$, $\mathbf{E}_0 = (\theta_0, \psi_0, \phi_0)^\top$, $\boldsymbol{\omega}_0 = (\omega_{x0}, \omega_{y0})$, and $\mathbf{E}_f = (\theta_f, \psi_f, \phi_f)^\top$, $\boldsymbol{\omega}_f = (\omega_{xf}, \omega_{yf})$.

**$\lambda_1$-continuation.** The parameter $\lambda_1$ is used to act, by continuation, on the initial conditions, according to $\mathbf{E}(0) = \mathbf{E}^*(1-\lambda_1) + \mathbf{E}_0\lambda_1$ and $\boldsymbol{\omega}(0) = \boldsymbol{\omega}^*(1-\lambda_1) + \boldsymbol{\omega}_0\lambda_1$, where $E^*$ and $\boldsymbol{\omega}^*$ are

calculated using (14)-(16). The shooting function $G_{\lambda_1}$ for the $\lambda_1$-continuation is given by

$$\begin{aligned} G_{\lambda_1} =& \big(v_z(t_f)\sin\psi_f + v_y(t_f)\cos\theta_f\cos\psi_f,\ v_z(t_f)\sin\theta_f - v_x(t_f)\cos\theta_f \\ & p_{vy}(t_f)\sin\psi_f - (p_{vx}(t_f)\sin\theta_f\cos\psi_f + p_{vz}(t_f)\cos\theta_f\cos\psi_f), \\ & p_r(t_f),\, p_\omega(t_f),\, p_E(t_f),\, H(t_f),\, \{z_i(t_i^-) = z_i(t_i)^+, i = 1,\cdots,N-1\}\big). \end{aligned}$$

Initializing with the solution of (**OCP0**), we solve this shooting problem with $\lambda_1 = 0$, and we get a solution of the problem (**EPUP**) with the terminal conditions (15)-(16) (the other states at $t_f$ being free). Then, by continuation, we make $\lambda_1$ vary from 0 to 1, and in this way we get, for $\lambda_1 = 1$, the solution of the problem (**EPUP**) with the terminal conditions (8) and (16). With this solution, we integrate the extremal equations (4)-(6) and (11) to get the values of the state variable at $t_i$, $i = 1,\cdots,N-1$ and $t_f$. We denote by $\mathbf{E}_e = (\theta(t_f), \psi(t_f), \phi(t_f))$ and $\boldsymbol{\omega}_e = (\omega_x(t_f), \omega_y(t_f))$ the "natural" conditions obtained at the final time.

**$\lambda_2$-continuation.** In a second step, we use the continuation parameter $\lambda_2$ to act on the final conditions, in order to make them pass from the "natural" values $\mathbf{E}_e$ and $\boldsymbol{\omega}_e$, to the desired target values $\mathbf{E}_f$, $\boldsymbol{\omega}_f$. The shooting function is

$$\begin{aligned} G_{\lambda_2} =& \big(v_z(t_f)\sin\psi_f + v_y(t_f)\cos\theta_f\cos\psi_f,\ v_z(t_f)\sin\theta_f - v_x(t_f)\cos\theta_f, \\ & p_{vy}(t_f)\sin\psi_f - (p_{vx}(t_f)\sin\theta_f\cos\psi_f + p_{vz}(t_f)\cos\theta_f\cos\psi_f), \\ & \mathbf{E}(t_f) - (1-\lambda_2)\mathbf{E}_e - \lambda_2\mathbf{E}_f,\ \boldsymbol{\omega}(t_f) - (1-\lambda_2)\boldsymbol{\omega}_e - \lambda_2\boldsymbol{\omega}_f, \\ & p_r(t_f),\, H(t_f),\, \{z_i(t_i^-) = z_i(t_i)^+, i = 1,\cdots,N-1\}\big). \end{aligned} \tag{17}$$

Solving this problem by making vary $\lambda_2$ from 0 to 1, we obtain the solution of the problem (**EPUP**) with the desired terminal conditions (8)-(9).

**$\lambda_3$-continuation.** The parameter $\lambda_3$ is used to introduce aerodynamic forces and gravity acceleration in (4) and (6), according to

$$\begin{aligned} \dot v_x &= a\sin\theta\cos\psi + g_{0x}(1-\lambda_3) + \lambda_3 g_x + \lambda_3\frac{D_x + L_x}{m}, \\ \dot v_y &= -a\sin\psi + g_{0y}(1-\lambda_3) + \lambda_3 g_y + \lambda_3\frac{D_y + L_y}{m}, \\ \dot v_z &= a\cos\theta\cos\psi + g_{0z}(1-\lambda_3) + \lambda_3 g_z + \lambda_3\frac{D_z + L_z}{m}, \end{aligned}$$

and $\rho(t) = \rho_0\big((1-\lambda_3)\exp(-(\|\mathbf{r}_d(0)\| - R_E)/h_s) + \lambda_3\exp(-(\|\mathbf{r}_d(t)\| - R_E)/h_s)\big)$, where $g_x$, $g_y$ and $g_z$ are given by (5), $(\mathbf{g}_0)_R = (g_{x0}, g_{y0}, g_{z0})^\top$, and $h_s = 7143$, $\rho_0 = 1.225$. Applying the PMP, the equations of the adjoint variable $p$ also involve $\lambda_3$. The shooting function is

$$\begin{aligned} G_{\lambda_3} =& \big(v_z(t_f)\sin\psi_f + v_y(t_f)\cos\theta_f\cos\psi_f,\ v_z(t_f)\sin\theta_f - v_x(t_f)\cos\theta_f, \\ & p_{vy}(t_f)\sin\psi_f - (p_{vx}(t_f)\sin\theta_f\cos\psi_f + p_{vz}(t_f)\cos\theta_f\cos\psi_f), \\ & \mathbf{E}(t_f) - \mathbf{E}_f,\ \boldsymbol{\omega}(t_f) - \boldsymbol{\omega}_f,\ p_r(t_f),\ H(t_f),\ \{z_i(t_i^-) = z_i(t_i)^+, i = 1,\cdots,N-1\}\big). \end{aligned} \tag{18}$$

This step is a continuation on the dynamics of the system, and the parameter $\lambda_3$ does not explicitly appear in the shooting function. By making the parameter $\lambda_3$ vary from 0 to 1, we get the solution of **(UPUP)**.

**$\lambda_4$-continuation and $K_p$-continuation.** Finally, the parameter $\lambda_4$ is used to act on the terms induced by the penalty function, in the Hamiltonian

$$H_{Kp} = \langle p(t), f(x(t))\rangle + u_1(t)\langle p(t), g_1(x(t))\rangle + u_2(t)\langle p(t), g_2(x(t))\rangle - (1 + K\|u\|^2 + \lambda_4 K_p P(x)),$$

The shooting function $G_{\lambda_4}$ is defined by replacing $H(t_f)$ with $H_{Kp}(t_f)$ in the shooting function $G_{\lambda_3}$ given by (18). Making $\lambda_4$ vary from 0 to 1, we obtain the solution of $\mathbf{(PUP)}_K$ with the penalty parameter $K_p = K_{p0}$. As said in Remark 1, a complementary continuation on $K_p$ from $K_{p0}$ to $K_{p1}$ is then required to retrieve a solution for which the path constraints are satisfied in an acceptable way. Moreover, as already mentioned, we can continue to decrease the value of $K$ in order to approach the solution of $\mathbf{(PUP)}_{K=0}$. This is an optional continuation step.

To implement efficiently the above four-parameter continuation, we use the PC continuation method combined with the multiple shooting method. However, we use two additional numerical tricks in order to improve the robustness of the algorithm and to tackle Euler singularities (see Section 2.1).

### 3.3 Change of Frame

Changing the reference frame can improve the problem conditioning and enhance the numerical solution process. The new frame $S'_R$ is designed by adequately rotating the initial frame $S_R$. This is a nonlinear state transformation, leading to a preconditioner that makes the proposed continuation procedure more robust. More precisely, we define the new coordinate $S_{R'}$ by two single-axis rotations from the frame $S_R$, given by

$$S_R \xrightarrow{R_y(\beta_1)} \circ \xrightarrow{R_x(\beta_2)} S_{R'},$$

and the transition matrix from $S_R$ to $S'_R$ is $L_{R'R} = R_x(\beta_2)R_y(\beta_1)$. Denoting the Euler angles of $S_b$ with respect to the new frame $S_{R'}$ as $\mathbf{E}' = (\theta', \psi', \phi')$, the transition matrix from $S'_R$ to $S_b$ is $L_{bR'} = R_z(\phi')R_x(\psi')R_y(\theta')$.

Using that $L_{bR}L_{RR'} = R_z(\phi)R_x(\psi)R_y(\theta)L_{R'R}^{\top} = L_{bR'}$, the angles $\mathbf{E}'$ are functions of $\mathbf{E}$, $\beta_1$, and $\beta_2$. Moreover, the velocity vector $\mathbf{v}$ in the $S'_R$ can also be obtained by $(\mathbf{v})'_R = L_{R'R}(\mathbf{v})_R$. The angular velocity vector $\boldsymbol{\omega}$ is expressed in the body frame $S_b$ and it is therefore not altered by this coordinate change.

Given fixed $\beta_1$ and $\beta_2$, the change of frame corresponds to the nonlinear invertible change of state variable $x' = \mathrm{diag}(L_{R'R}(\mathbf{r})_R, L_{R'R}(\mathbf{v})_R, \varphi_{att}(x), \mathbf{Id})$, where $\varphi_{att}(\cdot)$ maps Euler angles in $S_R$ to Euler angles in $S'_R$, i.e., $\mathbf{E}' = \varphi_{att}(x)$, and $\mathbf{Id}$ is the 3-dimensional identity matrix.

This state transformation can be seen as a preconditioner for our numerical method. Indeed, we use a Newton-like method to solve the boundary value problem in the shooting method. Let us for instance consider the simplest Newton method and let us denote by $Z$ the variables of the shooting method. Given an initial guess of $Z = Z_0$, the equation $G(Z) = 0$ is solved iteratively according to $J(Z_k)Z_{k+1} = J(Z_k)Z_k - G(Z_k)$, where $J = \partial G/\partial Z$. Define a diffeomorphism $\varphi(\cdot)$ such that $Z = \varphi(y)$. Then the original problem consists of solving $G(y) = 0$ and the Newton method iterative step becomes $J(y_k)y_{k+1} = J(y_k)y_k - G(y_k)$, where $J(y_k) = J(Z_k)\frac{\partial Z}{\partial y}(y_k)$. The matrix $M = (\frac{\partial Z}{\partial y})^{-1}$ actually acts as a preconditioner in the shooting method and it can be used to reduce the condition number of the Jacobian matrix $J$. In numerical experiments, we use the Fortran subroutine `hybrd.f` (see [37]) which uses a modification of the Powell hybrid method : the choice of the correction is a convex combination of the Newton and scaled gradient directions, and the updating of the Jacobian by the rank-1 method of Broyden.

Note in addition that the differential equations for the new variable $x'$ keep the same form as for the old variable $x$, and by using the PMP, the adjoint vector $p'$ to the new state $x'$ can also be

derived from $(x, p)$, according to

$$p'_r = L_{R'R} p_r, \quad p'_v = L_{R'R} p_v, \quad p'_E = \left( \frac{d\varphi_{att}(x)}{dx} \right)^{-1\top} p_E, \quad p'_\omega = p_\omega.$$

To sum up, the new reference frame $S'_R$ can be chosen such that the problem $\mathbf{(PUP)}_K$ is easier to solve numerically. However, a priori, we do not know what values $(\beta_1, \beta_2)$ are the most suitable. We propose to choose the pair such that $\psi'_f = -\psi'_0$ and $|\psi'_f| + |\psi'_0|$ being minimal. By doing this, the terminal values on the yaw angle are closer to the origin and hence farther from Euler singularities (see Section 2.1). We observe from numerical experiments that this choice enhances the algorithm robustness.

### 3.4 Euler singularities

Smoothing the vector fields at singular points of Euler angles also helps to tackle singularities. Assuming that $\dot{\theta}$ is bounded, we have $\omega_x \sin\phi + \omega_y \cos\phi \to 0$ when $\psi \to \pi/2 + k\pi$. Since $\dot{\theta}\dot{\phi} = \lim_{\psi \to \pi/2+k\pi} (\omega_x \sin\phi + \omega_y \cos\phi)^2 \sin\psi \to 0$ and $\dot{\theta}/\dot{\phi} \to 1$ as $\psi \to \pi/2 + k\pi$, it follows that $\dot{\theta} = \dot{\phi} = 0$ as $\psi \to \pi/2 + k\pi$. Assuming that $-\frac{p_\theta + p_\phi \sin\psi}{\cos\psi} \to A < \infty$ as $\psi \to \pi/2 + k\pi$, it follows from the fact that

$$A = \lim_{\psi \to \pi/2+k\pi} -\frac{p_\theta + p_\phi \sin\psi}{\cos\psi} = \lim_{\psi \to \pi/2+k\pi} \frac{\dot{p}_\theta + \dot{p}_\phi \sin\psi + p_\phi \cos\psi \dot{\psi}}{\sin\psi \dot{\psi}} = -A$$

that $A = 0$. Hence, we get $\dot{p}_\theta = 0$, $\dot{p}_\phi = 0$, $\dot{p}_\psi = a \sin\theta p_{vx} + a \cos\theta p_{vz}$, $\dot{p}_{\omega_x} = -p_\psi \cos\phi$, $\dot{p}_{\omega_y} = p_\psi \sin\phi$. Summing up, at points $\psi \to \pi/2 + k\pi$, (4) and (11) become

$$\begin{aligned} &\dot{\theta} = 0, \quad \dot{\psi} = \omega_x \cos\phi - \omega_y \sin\phi, \quad \dot{\phi} = 0, \quad \dot{\omega}_x = -\bar{b} u_2, \quad \dot{\omega}_y = \bar{b} u_1, \\ &\dot{p}_\theta = 0, \quad \dot{p}_\psi = a \sin\theta p_{v_x} + a \cos\theta p_{v_z}, \quad \dot{p}_\phi = 0, \quad \dot{p}_{\omega_x} = -p_\psi \cos\phi, \quad \dot{p}_{\omega_y} = p_\psi \sin\phi. \end{aligned} \tag{19}$$

When we are close to a singularity, we rather use (19).

### 3.5 Algorithm

We describe the whole numerical strategy in the following algorithm.

**Result**: The solution of the problem $\mathbf{(PUP)}_K$
· Change of frame : compute $(\beta_1, \beta_2)$ and the new initial condition $x(0) = x_0'$ (Section 3.3);
· Solve **(OCP0)** to get a solution $Z_0$;
· Initialize the multiple shooting method with $Z_0$ and $\lambda_i = 0$, $i = 1, \cdots 4$;
**for** $i = 1, \cdots, 4$ **do**
  **while** $\lambda_i \leqslant 1$ *and* $\triangle\lambda^i_{min} \leqslant \triangle\lambda_i \leqslant \triangle\lambda^i_{max}$ **do**
    (Predictor) Predict a point $(\tilde{Z}, \tilde{\lambda}_i)$ according to (13);
    (Corrector) Find the solution $(\bar{Z}, \bar{\lambda}_i)$ of $G_{\lambda i}(\tilde{Z}, \tilde{\lambda}_i) = 0$;
    **if** *successful* **then**
      $(Z, \lambda_i) = (\bar{Z}, \bar{\lambda}_i)$;
    **else**
      Choose a new step-length $h_s$ ;
    **end**
  **end**
  **if** *successful* **then**
    The $\lambda_i$-continuation is successful;
  **else**
    The $\lambda_i$-continuation failed;
  **end**
**end**

**Algorithm 1:** Prediction-Corrector continuation

## 4 Numerical results

In this section, we solve $\mathbf{(PUP)}_K$ using the algorithm proposed in Section 3.5. We first present a pull-up maneuver of an ALV just after its release from the airplane and we present some statistical results showing robustness of our algorithm. Then we apply the algorithm to the three-dimensional reorientation maneuver of the upper stage of a LV after a stage separation.

### 4.1 Pull-up maneuvers of the AVL

We consider a pull-up maneuver of an ALV.

The data used in (4) and (6) approximate a Pegasus-like airborne launcher : $a = 15.8$, $b = 0.2$, $S = 14\,m^2$, $C_{x0} = 0.06$, $C_{x\alpha} = 0$, $C_{z0} = 0$, $C_{z\alpha} = 4.7$. Let $\bar{n}_{max} = 2.2g$ and $\bar{q}_{max} = 47\,kPa$. The initial conditions (8) are

$$r_{x0} = 11.9\,km, \quad r_{y0} = r_{z0} = 0, \quad v_0 = 235\,m/s, \quad \theta_{v0} = -10^\circ,$$

$$\psi_{v0} = 0^\circ, \quad \theta_0 = -10^\circ, \quad \psi_0 = \phi_0 = 0, \quad \omega_{x0} = \omega_{y0} = -1^\circ/s,$$

and the final conditions (9) are

$$\theta_f = 42^\circ, \quad \psi_f = 10^\circ, \quad \phi_f = 0, \quad \omega_{xf} = \omega_{yf} = 0.$$

Note that generally the pull-up maneuvers are planar ($\psi_f = 0^\circ$). Here we set $\psi_f = 10^\circ$ with the aim of showing that the algorithm can also deal efficiently with the non-planar pull-up maneuvers ($\psi_f \neq 0^\circ$).

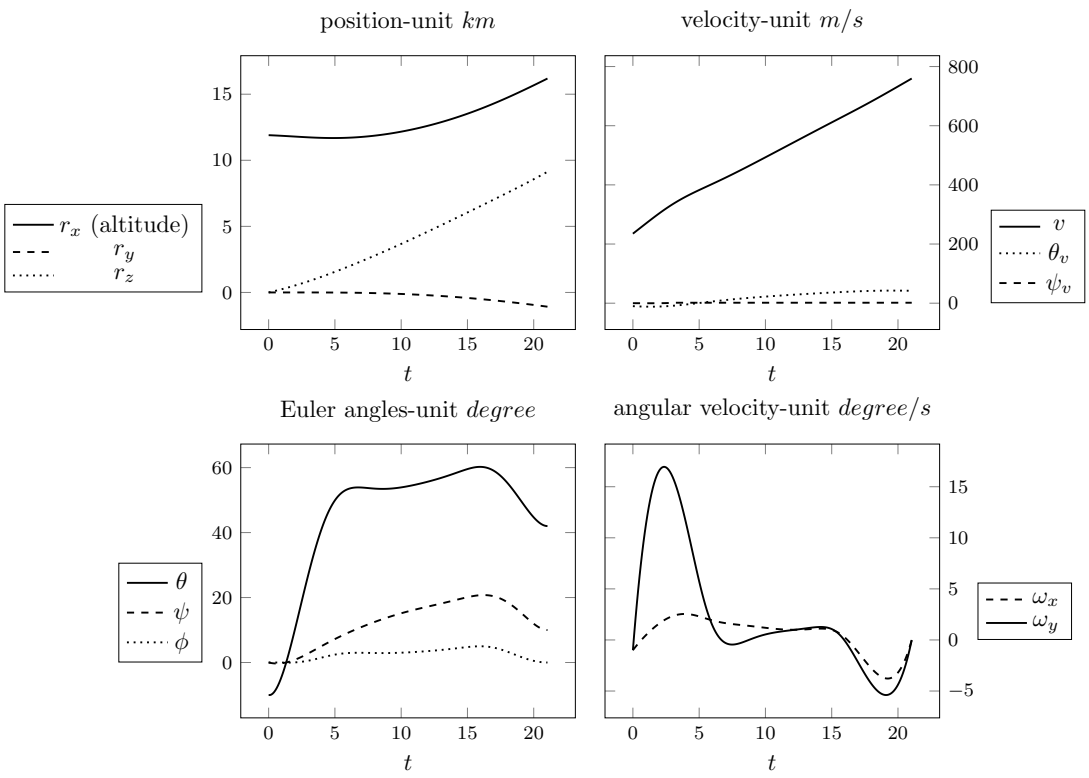


FIGURE 3 – Time history of state variable $x(t)$ for an ALV.

The multiple shooting method is applied with three node points. The components of the state variable $x$ and the control $u$ are reported on Figs 3 and 4. The components $p_{\omega_x}$, $p_{\omega_y}$ and $p_\theta$ of the adjoint variable $p$ are given on Fig. 4. The time histories of the load factor $\bar{n}$ and of the dynamic pressure $\bar{q}$ are reported on Fig. 5.

From Fig. 5 (left), we see that there is a boundary arc of the load factor constraint. According to the $p_{\omega_y}(t)$ in Fig. 4 (right), we see that, over the boundary arc, the switching function $h(t) = b(p_{\omega_y}, -p_{\omega_x})$ indeed stays close to zero. Comparing the two subfigures of Fig. 4, we see that the control follows the form of the switching function. Moreover, the path constraint of the dynamic pressure is not active.

As mentioned in Remark 1, the large value of $K_p$ often causes numerical difficulties. In this example, we observe on Fig. 4(right) that, at $t = 5.86\,s$, the curve $p_\theta(t)$ is not as smooth as the other parts. Indeed, at $t = 5.86\,s$, the penalty function $P(x)$ starts to be positive and thus provides nonzero terms in the adjoint differential equation.

Running this example requires $24.6\,s$ to compute the optimal solution, with CPU : Intel(R) Core(TM) i5-2500 CPU 3.30GHz ; Memory : 3.8 Gio ; Compiler : gcc version 4.8.4 (Ubuntu 14.04 LTS). If the multiple shooting method is applied with four node points, the computing time is $31.2\,s$. Actually, this example takes a bit longer time since we have required a non-planar maneuver. For a planar maneuver, the computing time is about $20\,s$ (see Table 2).

In the following, we present some statistical results done with the same computer settings.

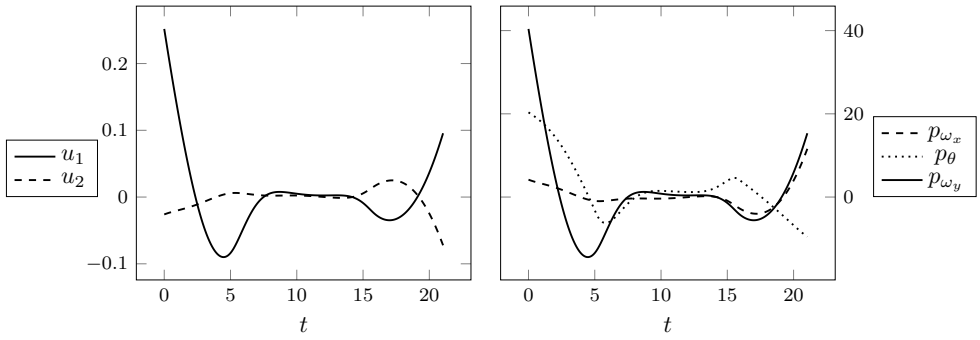


FIGURE 4 – Time history of control variable $u(t)$ and adjoint variable $p_{\omega_x}$, $p_{\omega_y}$, $p_\theta$ for an ALV.

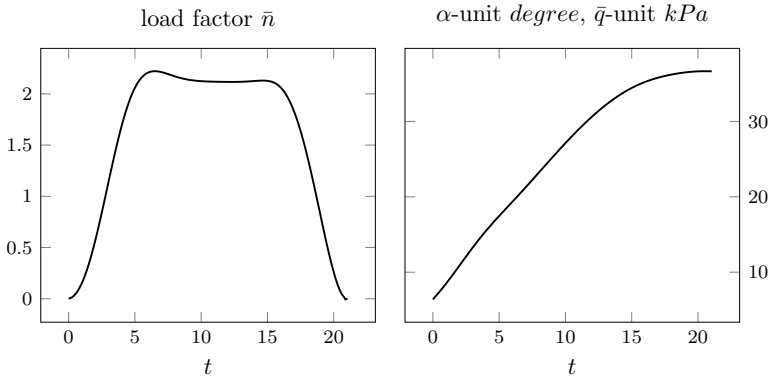


FIGURE 5 – Time history of the constraints $c(x(t))$ for an ALV.

**Statistical results** We solve $\mathbf{(PUP)}_K$ with different terminal conditions. Initial and final conditions are swept in the range given in Table 1. The last cell of the table defines the restriction applied to the terminal conditions in order to exclude unrealistic cases. For each variable, we choose a discretization step and we solve all possible combinations of this discretization (factorial experiment). There are 1701 cases.

TABLE 1 – Parameter ranges.

| $v_0$ | $\theta_{v0}$ | $\psi_{v0}$ | $\theta_0$ | $\psi_0$ |
|---|---|---|---|---|
| fixed $0.8\,Ma$ | $[-10, 0]°$ | fixed $0°$ | $[-10, 10]°$ | fixed $0°$ |
| $\theta_f$ | $\psi_f$ | $\omega_{x0}$ | $\omega_{y0}$ | $\theta_0 - \theta_{v0}$ |
| $[20, 80]°$ | $[-10, 10]°$ | $[-2, 2]°/s$ | $[-2, 2]°/s$ | $[0, 10]°$ |

Statistical results are reported in Table 2. The multiple shooting method is applied with two node points. Set $K = 1 \times 10^3$, $K_{p0} = 0.1$ and $K_{p1} = 100$. We see from the results that the algorithm is robust with respect to terminal conditions and that it is rather fast in comparison with a simple direct method. Note that the choice of the regularisation parameter $K$ affects importantly the resolution results.

TABLE 2 – Statistical results.

| Statistical results | | |
|---|---|---|
| | planar | non-planar |
| Number of cases | 567 | 1134 |
| Rate of success (%) | 91.0 | 90.5 |
| Average execution time (s) | | |
| - Total | 20.9 | 46.2 |
| - In $\lambda_1$-continuation | 0.36 | 0.32 |
| - In $\lambda_2$-continuation | 1.27 | 1.44 |
| - In $\lambda_3$-continuation | 2.27 | 3.46 |
| - In $\lambda_4$-continuation | 17.23 | 40.75 |
| Average number of simulations | | |
| - Total | 150.3 | 229.3 |
| - In $\lambda_1$-continuation | 51.1 | 14.9 |
| - In $\lambda_2$-continuation | 17.5 | 28.0 |
| - In $\lambda_3$-continuation | 16.7 | 25.7 |
| - In $\lambda_4$-continuation | 65.0 | 160.7 |

## 4.2 Rapid attitude maneuver of the LVs

We note that, when solving the multi-burn ascent problem for LVs (see [5, 17, 20, 23]), it is possible to find a control (Euler angles) that contains a jump between different stages (see for example [33, Fig. 3]). In this case, a rapid attitude maneuver has to be done such that the LV can follow the optimal trajectory of the next stage. For this reason, we apply the presented algorithm as well to the maneuver problem of the upper stages of the LVs.

In contrast to the ALV's pull-up maneuver, these attitude maneuvers are in general three-dimensional and of lower magnitude. They occur at high altitudes (typically higher than 50 km) since a sufficiently low dynamic pressure is required to ensure the separation safety. In addition, compared to ALV, the velocity of in this case is in general much larger.

In this case, the path constraints are not active due to the low dynamic pressure, and we are rather interested in obtaining the fastest possible maneuver. To this aim, we need to decrease the parameter $K$, as shown in Fig. 2.

In the example, we set the system parameters in (4) and (6) to $a = 20$, $b = 0.2$, which approximate an Ariane-like launcher. The initial conditions (8) are

$$r_{x0} = 100\,km, \quad r_{y0} = r_{z0} = 0, \quad v_0 = 5000\,m/s, \quad \theta_{v0} = 30^\circ,$$

$$\psi_{v0} = 0^\circ, \quad \theta_0 = 40^\circ, \quad \psi_0 = \phi_0 = 0, \quad \omega_{x0} = \omega_{y0} = 0,$$

and the final conditions (9) are

$$\theta_f = 60^\circ, \quad \psi_f = 10^\circ, \quad \phi_f = 0, \quad \omega_{xf} = \omega_{yf} = 0.$$

The multiple shooting method is applied with four node points. On Figs 6 and 7, we report the components of state and control variables. We observe that, when $t \in [32, 145]\,s$, the control is very small, and the state variable $\theta = 151.5^\circ \approx \theta^* = 151.57^\circ$, $\psi = 8.6^\circ \approx \psi^* = 8.85^\circ$ with $\theta^*$ and $\psi^*$ calculated by (14). Indeed, the control in Fig. 7 is continuous thanks to the regularization term $K \int_0^{t_f} \|u\|^2 dt$ in the cost functional. It helps to generate a solution and to avoid chattering [51, 52].

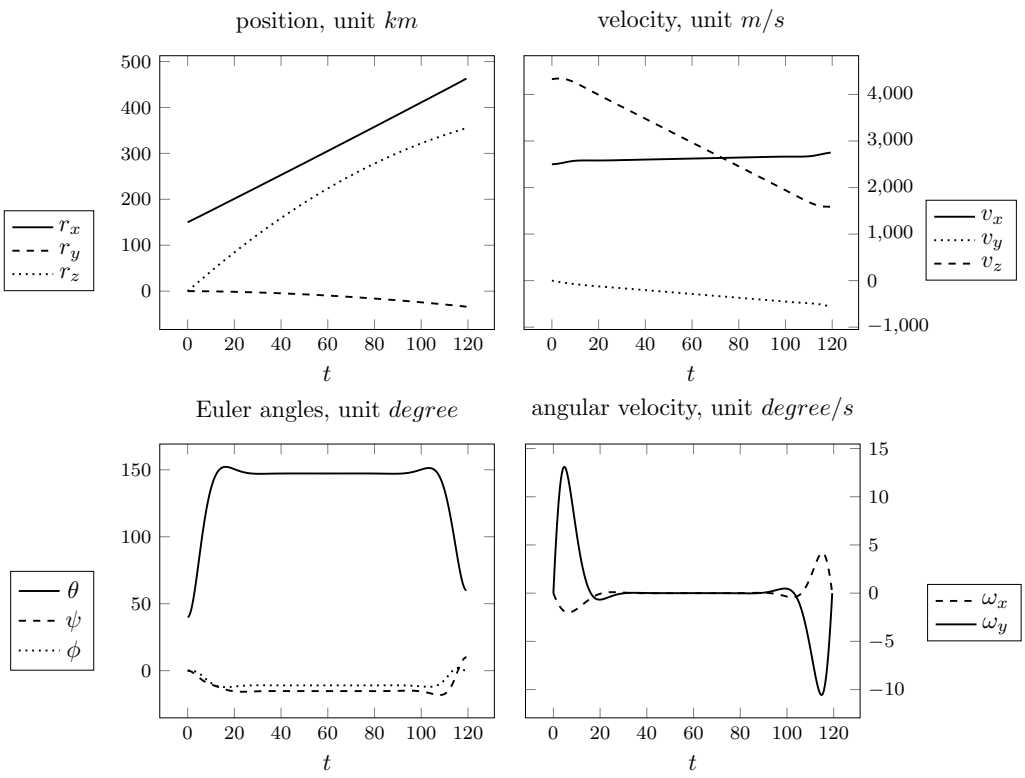


FIGURE 6 – Time history of state variable $x(t)$ for a LV.

In the presented result, we have started with $K = 8 \times 10^4$ and stopped with $K = 240$ and the computing time is about $110\,s$. This maneuver time $t_f$ is about $120\,s$, due to the fact that we require as well the direction of the trajectory velocity to change as much as the Euler angles. While for real LVs, only minor adjustment of velocity direction is needed while doing a large attitude maneuver. Therefore, in practice, the maneuver time is in general only several seconds. Our aim of presenting this "non-realistic" case is indeed to show that the proposed algorithm is also robust to a large range of system configurations and quite extreme terminal conditions.

# 5 Conclusion

In this paper, we have addressed the problem of minimum time-energy pull-up maneuver problem for ALVs. The dynamics couple attitude and trajectory motion. Our algorithm combines an indirect approach with a multi-parameter numerical continuation procedure. Starting from the explicit solution of a simplified problem of lower dimension, the successive continuations consist of retrieving the true dynamics and terminal conditions. With two continuation parameters, the terminal conditions are successively retrieved. Aerodynamic forces and variable gravity are then introduced with a third continuation parameter. Finally, the state constraints are applied with other continuations. The multiple shooting method, the PC continuation method, the change of reference frame and the smoothing of vector fields are also employed to improve numerical stability and robustness of the algorithm. An example of the pull-up maneuver for an ALV is given and statistical experiments show that our approach is fast and robust. In addition, the application

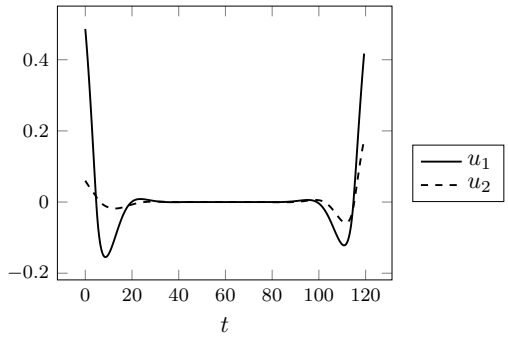


FIGURE 7 – Time history of control variable $u(t)$ for a LV.

for the rapid maneuver of an upper stage for a LV is exemplified numerically. Indeed, with this algorithm, the solution of similar classes of problems can be obtained from scratch in a quite short time, whatever the launcher data and the terminal conditions are.

**Acknowledgment.** The second author acknowledges the support by FA9550-14-1-0214 of the EOARD-AFOSR.

# Références

[1] E.L. Allgower, K. Georg, Numerical continuation methods : an introduction, *Springer Science & Business Media*, 2012.

[2] Ardema, M. , Nonlinearly singularly perturbed optimal control problems with singular arcs, *Automatica*, 1980, Vol. 1, No. 16, pp 99–104.

[3] Bérend, N., Bourgaie, M., Defoort, S., Hermetz, J., Le Tallec, C., Bec, R., Innovative Air-Launch System Using a Multirole UAV. *In 57th International Astronautical Congress*, Valence, Spain, 2006.

[4] Bradt, J. E., Jessick, M. V., Hardtla, J. W. , Optimal guidance for future space applications, *AIAA paper*, 1987, pp. 87–2401.

[5] Brown, K. R., Harrold, E. F., Johnson, G. W., Rapid optimization of multiple-burn rocket trajectories, *NASA CR-1430*, September, 1969.

[6] van Buren, M. A., Mease, K. D., Aerospace plane guidance using time-scale decomposition and feedback linearization, *Journal of guidance, control, and dynamics*, 1992, Vol. 5, No. 15, pp. 1166–1174.

[7] J.B. Caillau, O. Cots, et J. Gergaud, Differential continuation for regular optimal control problems. *Optimization Methods and Software*, 2012, vol. 27, no 2, pp. 177–196.

[8] J.B. Caillau, B. Daoud Minimum time control of the restricted three-body problem, *SIAM Journal on Control and Optimization*, 2012, vol. 50, no 6, pp. 3178–3202.

[9] Calise, A. J., Melamed, N., Lee, S., Design and evaluation of a three-dimensional optimal ascent guidance algorithm, *Journal of Guidance, Control, and Dynamics*, 1998, Vol. 21, No. 6, pp. 867–875.

[10] Cerf, M., Haberkorn, T., Trélat, E., Continuation from a flat to a round Earth model in the coplanar orbit transfer problem, *Optimal Control Appl. Methods*, 2012, Vol. 33, no. 6, pp. 654–675.

[11] Clegern, J. B., Ostrander, M. J., Pegasus upgrades - A continuing study into an air-breathing alternative. *In 31 st AIAA, ASME, SAE, and ASEE, Joint Propulsion Conference and Exhibit*, San Diego, CA, 1995.

[12] Corban, J. E., Calise, A. J., Flandro, G. A., Rapid near-optimal aerospace plane trajectory generation and guidance, *Journal of guidance, control, and dynamics*, 1991, Vol. 6, No. 14, pp. 1181–1190.

[13] Corvin, M. A., Ascent guidance for a winged boost vehicle, *NASA CR-172083*, August, 1988.

[14] Denham, W. F., Bryson, A. E., Optimal programming problems with inequality constraints. 2. Solution by steepest-ascent, *AIAA JOURNAL*, 1964, Vol. 1, No. 2, pp. 25–34.

[15] Dukeman, G. A., Atmospheric ascent guidance for rocket-powered launch vehicles, *AIAA paper*, 2002, Vol. 4559, pp. 5-8.

[16] Dukeman, G., Calise, A. J., Enhancements to an atmospheric ascent guidance algorithm, *AIAA paper*, 2003, Vol. 5638.

[17] Dukeman, G. A., Hill, A., Rapid trajectory optimization for the Ares I launch vehicle, *AIAA Paper*, 2008, Vol. 6288.

[18] A. T. Fuller, An optimum non-linear control system, *In the Proceedings of IFAC Congress*, 1961, Moscow, USSR.

[19] C. Frangos, J.A. Snyman, The application of parameter optimisation techniques to linear optimal control system design. *Automatica*, 1992, vol. 28, no 1, pp. 153–157.

[20] Gath, P. F., Calise, A. J., Optimization of launch vehicle ascent trajectories with path constraints and coast arcs, *Journal of Guidance, Control, and Dynamics*, 2001, Vol. 2, No. 24, pp. 296–304.

[21] J. Gergaud, T. Haberkorn, P. Martinon, Low thrust minimum fuel orbital transfer : an homotopic approach, *Journal of Guidance, Control and Dynamics*, 2004, Vol. 27, No. 6, pp. 1046–1060.

[22] R.F. Hartl, S.P. Sethi, R.G. Vickson, A survey of the maximum principles for optimal control problems with state constraints. *SIAM review*, 1995, vol. 37, no 2, pp. 181-218.

[23] Jezewski, D. J., Optimal analytic multiburn trajectories. *AIAA Journal*, 1972, Vol. 5, No. 10, pp. 680–685.

[24] Kamm, Y., Gany, A., Solid rocket motor optimization, *In 44th AIAA/ASME/SAE/ASEE Joint Propulsion Conference & Exhibit*, 2008, pp. 4695.

[25] van Kesteren, M. W., Zandbergen, B. T. C., Naeije, M. C., van Kleef, A. J. P., Design and analysis of an airborne, solid propelled, nanosatellite launch vehicle using multidisciplinary design optimization, 2015

[26] Kremer, J. P., Mease, K. D. , Near-optimal control of altitude and path angle during aerospace plane ascent, *Journal of guidance, control, and dynamics*, 1997, Vol. 4, No. 20, pp. 789–796.

[27] Lee, K. S., Sarigul-Klijn, N., Computational prediction and comparison of ground versus air launched rocket noise, *43rd AIAA/ASME/SAE/ASEE Joint Propulsion Conference & Exhibit*, 2007.

[28] Leung, M. S., Calise, A. J., Hybrid approach to near-optimal launch vehicle guidance, *Journal of Guidance, Control, and Dynamics*, 1994, Vol. 5, No. 17, pp. 881–888.

[29] Lu, P., Sun, H., Tsai, B., Closed-loop endoatmospheric ascent guidance, *Journal of Guidance, Control, and Dynamics*, 2003, Vol. 2, No. 26, pp. 283-294.

[30] Lu, P., Griffin, B. J., Dukeman, G. A., Chavez, F. R., Rapid optimal multiburn ascent planning and guidance, *Journal of Guidance, Control, and Dynamics*, 2008, Vol. 6, No. 31, pp. 1656–1664.

[31] Pan, B., Lu, P., Rapid optimization of multiburn rocket trajectories revisited, *AIAA Paper*, 2009, Vol. 6105, pp. 10–13.

[32] Lu, P., Pan, B., Highly constrained optimal launch ascent guidance, *Journal of guidance, control, and dynamics*, 2010, Vol. 2, No. 33, pp. 404–414.

[33] Lu, P., Forbes, S., Baldwin, M., A versatile powered guidance algorithm, *In AIAA Guidance, Navigation, and Control Conference*, 2012, pp. 4843.

[34] C. Marchal, Chattering arcs and chattering controls, *Journal of Optimization Theory and Applications*, 1973, Vol. 11, No 5, pp. 441–468.

[35] Markopoulos, N., Calise, A., Near-optimal, asymptotic tracking in control problems involving state-variable inequality constraints, *In AIAA Guidance, Navigation and Control Conference*, Monterey, California, 1993.

[36] P. Martinon, J. Gergaud, Using switching detection and variational equations for the shooting method, *Optimal Control Applications and Methods*, 2007, Vol. 28, No. 2, pp. 95–116.

[37] J.J. Moré, D.C. Sorensen, K.E. Hillstrom, et al. The MINPACK project. *Sources and Development of Mathematical Software*, 1984, pp. 88–111.

[38] Mosier, M. R., Harris, G. N., Whitmeyer, C., Pegasus air-launched space booster payload interfaces and processing procedures for small optical payloads, *In Orlando'91, Orlando, FL (pp. 177-192), International Society for Optics and Photonics*, 1991.

[39] Naidu, D. S., & Calise, A. J., Singular perturbations and time scales in guidance and control of aerospace systems : A survey, *Journal of Guidance, Control, and Dynamics*, 2001, Vol. 6, No. 24, pp. 1057–1078.

[40] Pan, B., Lu, P., Improvements to optimal launch ascent guidance, *AIAA Paper*, 2010, Vol. 8174, pp 2–5.

[41] Pontryagin, L.S., Mathematical theory of optimal processes, *CRC Press*, 1987.

[42] Robbins, H. M. , Optimality of intermediate-thrust arcs of rocket trajectories, *AIAA Journal*, 1965, Vol. 6, No. 3, pp. 1094–1098.

[43] Roble, N. R., Petters, D. P., Fisherkeller, K. J., Further exploration of an airbreathing Pegasus alternative, *In Joint Propulsion Conference and Exhibit*, 1993, Vol. 1.

[44] Sarigul-Klijn, M., Sarigul-Klijn, N., A study of air launch methods for rlvs, *AIAA Paper*, 2001.

[45] Sarigul-Klijn, N., Noel, C., Sarigul-Klijn, M., Air launching earth-to-orbit vehicles : Delta V gains from launch conditions and vehicle aerodynamics, *AIAA*, 2004, Vol. 872.

[46] Sarigul-Klijn, N., Sarigul-Klijn, M., Noel, C, Air-launching earth to orbit : effects of launch conditions and vehicle aerodynamics. *Journal of spacecraft and rockets*, 2005, Vol. 3, No. 42, pp 569–575.

[47] J.A. Snyman, N. Stander, W.J. Roux, A dynamic penalty function method for the solution of structural optimization problems, *Applied Mathematical Modelling*, 1994, vol. 18, no 8, pp. 453–460.

[48] Trélat, E., Optimal control and applications to aerospace : some results and challenges, *Journal of Optimization Theory and Applications*, 2012, Vol. 154, No. 3, pp. 713–758.

[49] Trélat, E., Zuazua, E., The turnpike property in finite-dimensional nonlinear optimal control, *J. Differential Equations*, 2015, Vol. 258, No. 1, pp. 81–114.

[50] M.I. Zelikin, V.F. Borisov, A.J. Krener, Theory of Chattering Control : with applications to Astronautics, Robotics, Economics, and Engineering, *Springer*, 1994.

[51] Zhu, J., Trélat, E., Cerf, M., Planar tilting maneuver of a spacecraft : singular arcs in the minimum time problem and chattering, *Preprint arXiv :1504.06219*, 2015, 43 pages, to appear in Discrete Cont. Dynam. Syst. Ser. B.

[52] Zhu, J., Trélat, E., Cerf, M., Minimum time control of the rocket attitude reorientation associated with orbit dynamics, *Preprint arXiv :1507.00172*, 2015, 33 pages, to appear in SIAM J. Cont. Optim.